

**Immuno-PET using anti-CEA bispecific antibody and <sup>68</sup>Ga-labeled peptide in metastatic medullary thyroid carcinoma: clinical optimization of the pretargeting parameters in a First-in Human trial.**

Caroline Bodet-Milin<sup>1,2</sup>, Alain Faivre-Chauvet<sup>1,2</sup>, Thomas Carlier<sup>1,2</sup>, Aurore Rauscher<sup>2,3</sup>, Mickael Bourgeois<sup>1,2</sup>, Evelyne Cerato<sup>1</sup>, Vincent Rohmer<sup>4</sup>, Olivier Couturier<sup>5</sup>, Delphine Druil<sup>6</sup>, David M. Goldenberg<sup>7,8</sup>, Robert M. Sharkey<sup>8</sup>, Jacques Barbet<sup>2,9</sup>, Françoise Kraeber-Bodere<sup>1,2,3</sup>

<sup>1</sup>Nuclear Medicine, University Hospital, Nantes, France,

<sup>2</sup>CRCNA, Inserm U892, CNRS UMR 6299, Nantes, France,

<sup>3</sup>Nuclear Medicine, ICO Cancer Center, Saint-Herblain, France,

<sup>4</sup>Endocrinology Department, University Hospital, Angers, France,

<sup>5</sup>Nuclear Medicine, University Hospital, Angers, France,

<sup>6</sup>Endocrinology Department, University Hospital, Nantes, France,

<sup>7</sup>IBC Pharmaceuticals, Inc., Morris Plains, NJ, USA,

<sup>8</sup>Immunomedics, Inc., Morris Plains, NJ, USA,

<sup>9</sup>GIP Arronax, Saint-Herblain, France

Corresponding author: Caroline Bodet-Milin, Nuclear Medicine Department, Hôtel Dieu

University Hospital, 1 Place Ricordeau, 44093 Nantes, France

Tel: +33 240084136; Fax: +33 240084218 E-mail: caroline.milin@chu-nantes.fr

**Running Title: Pretargeted immuno-PET in MTC**

**Word counts: 4979**

## **ABSTRACT**

Earlier clinical studies reported a high sensitivity of pretargeted immunoscintigraphy using murine or chimeric anti-carcinoembryonic antigen (CEA) bispecific antibody (BsMAb) and peptides labeled with  $^{111}\text{In}$  or  $^{131}\text{I}$  in medullary thyroid carcinoma (MTC). Preclinical studies showed that new generation humanized recombinant anti-CEA x anti-histamine-succinyl-glycine (HSG) trivalent BsMAb TF2 and radiolabeled HSG peptide (IMP288) present good features for PET. This study aimed at optimizing molar doses and pretargeting interval of TF2 and  $^{68}\text{Ga}$ -labeled IMP288 for immuno-PET in relapsed MTC patients with calcitonin serum levels  $> 150$  pg/ml.

**Materials and methods** Five cohorts (C1 to C5) of 3 patients received variable molar doses of TF2 and  $\sim 150$  MBq  $^{68}\text{Ga}$ -IMP288 after different pretargeting time intervals (C1: 120 nmol TF2, 6 nmol IMP288, 24 h; C2: 120, 6, 30 h; C3: 120, 6, 42 h; C4: 120, 3, 30 h; C5: 60, 3, 30 h). TF2 and  $^{68}\text{Ga}$ -IMP288 pharmacokinetics were monitored. Whole-body PET was recorded 60 and 120 min after  $^{68}\text{Ga}$ -IMP288 injection. Tumor maximal standardized uptake value ( $\text{T-SUV}_{\text{max}}$ ) and  $\text{T-SUV}_{\text{max}}/\text{mediastinum blood pool (MBP) SUV}_{\text{mean}}$  ratios (T/MBP) were determined.

**Results** In C1,  $\text{T-SUV}_{\text{max}}$  and T/MBP ranged from 4.09 to 8.93 and 1.39 to 3.72 at 60 min and 5.14 to 11.25 and 2.73 to 5.38 at 120 min, respectively. Because of the high MBP, the delay was increased to 30 h in C2, increasing  $\text{T-SUV}_{\text{max}}$  and T/MBP. Further increasing the delay to 42 h in C3 decreased  $\text{T-SUV}_{\text{max}}$  and T/MBP, showing that 30 h was the most favorable delay. In C4, the TF2/peptide mole ratio was increased to 40 (delay 30 h), resulting in high  $\text{T-SUV}_{\text{max}}$  but with higher MBP than in C2. In C5 the molar dose of TF2 was reduced, resulting in lower imaging performance. Pharmacokinetic demonstrated a fast TF2 clearance and a clear relationship between blood activity clearance and the ratio between the molar amount of injected peptide to the molar amount of circulating TF2 at the time of peptide injection.

**Conclusion** High tumor uptake and contrast can be obtained with pretargeted anti-CEA immuno-PET in relapsed MTC patients, especially using optimized pretargeting parameters: BsMAb/peptide mole ratio of 20 and 30 h-pretargeting delay.

**Key Words** Medullary thyroid carcinoma, immuno-PET, pretargeting, bispecific antibody,  $^{68}\text{Ga}$ , pharmacokinetics

## INTRODUCTION

Medullary thyroid carcinoma is relatively infrequent, accounting for less than 10% of all thyroid cancers (1). After initial surgery, serum calcitonin is still detectable in nearly 20% of patients, suggesting residual disease and imaging, including neck ultrasonography, neck and chest computed tomography (CT), liver contrast-enhanced CT or magnetic resonance imaging (MRI) and spine and pelvis bone MRI, is recommended when serum calcitonine is higher than 150 pg/ml (1,2). With the ability to characterize and quantify cancer molecular processes,  $^{18}\text{F}$ -DOPA or  $^{18}\text{F}$ -FDG PET/CT also show high performance in relapsed MTC patients and great potential as a surrogate biomarker, useful for early response evaluation and prediction of clinical outcome (3–6).

MTC is characterized by an intense expression of CEA and previous clinical trials showed the high sensitivity of pretargeted immunoscintigraphy using murine or chimeric anti-CEA BsMAb and pretargeted haptens-peptides labeled with  $^{111}\text{In}$  or  $^{131}\text{I}$  (5,7,8). These results and the high potential of immuno-PET reported in other solid tumors using different radioimmunoconjugates suggested that pretargeted haptens labeled with PET emitters would allow high sensitivity and specificity imaging under good conditions of radiation protection and dosimetry (9,10).

Today, new pretargeting reagents have been designed (11–15). TF2 is an engineered trivalent BsMAb composed of a humanized anti-HSG Fab-fragment derived from the murine 679 antibody, and two humanized anti-CEA Fab-fragments derived from the hMN-14 antibody, formed into a 157 kD protein by the Dock-and-Lock<sup>®</sup> procedure (11). IMP288 is a bivalent HSG hapten that can be labeled with a variety of radionuclides for therapy ( $^{90}\text{Y}$  and  $^{177}\text{Lu}$ ), scintigraphy ( $^{111}\text{In}$ ) or PET ( $^{124}\text{I}$ ,  $^{68}\text{Ga}$  and  $^{18}\text{F}$ ). The clinical implementation of pretargeting requires a first phase to optimize the BsMAb and peptide molar doses and the delay between the two injections (14–17). The first clinical results were reported using TF2/ $^{177}\text{Lu}$ -IMP288 in colorectal carcinoma patients, showing fast tumor uptake and high tumor-to-background activity

ratios within a few hours (14). This feature is favorable for labeling with short-lived  $^{68}\text{Ga}$  and  $^{18}\text{F}$ , as confirmed by animal studies,  $^{68}\text{Ga}$  having the advantage of availability via a generator (13).

Thus, a study was designed in relapsed MTC patients to transfer into the clinic TF2 / $^{68}\text{Ga}$ -IMP288 pretargeting, with a first part to determine the best pretargeting parameters in different cohorts of patients injected with variable TF2 and IMP288 molar doses at variable pretargeting delays and a second part to assess immuno-PET performances. We report here the results of the optimization part of the study.

## **MATERIALS AND METHODS**

### **Population**

Patients  $\geq 18$  years with a histological diagnosis of MTC treated by complete surgery and presenting a calcitonin serum level  $\geq 150$  pg/ml with at least one lesion  $\geq 10$  mm on conventional imaging, were eligible. In the 4 weeks preceding immuno-PET, a staging workup that included a complete history, physical examination, CEA and calcitonin serum level measurement with biomarker doubling time determination when possible. As recommended by the international guidelines a contrast-enhanced CT of neck, chest, abdomen, and pelvis, a bone marrow MRI, and liver MRI were performed (2). A  $^{18}\text{F}$ -DOPA PET/CT was also performed to obtain an optimal disease staging. The other inclusion criteria were Karnofsky performance status  $\geq 70$  or Eastern Cooperative Oncology Group performance status 0-1, minimum life expectancy of 6 months, creatinine  $\leq 2.5$  x normal, normal serum human anti-mouse antibody (HAMA) and human anti-humanized antibody (HAHA) titers. Women of child-bearing potential must have a negative pregnancy test. The exclusion criteria were pregnancy and breast feeding, anti-cancer treatment within 6 weeks before immuno-PET or necessity to start anti-cancer treatment in the 3 months following immuno-PET, any serious active disease or co-morbid medical condition (according to the investigator's decision), any history of other cancer during the last 5 years, with the exception of non-melanoma skin tumors or stage 0 (in situ) cervical carcinoma, and a known hypersensitivity to antibodies or proteins. The trial sponsored by

Nantes University Hospital was approved by the responsible ethics committee (CPP), registered at ClinicalTrial.gov (NCT01730638) and all patients signed a written informed consent.

### **Investigational products and labeling**

The reagents were prepared suitable for human use by Immunomedics, Inc. (Morris Plains, NJ, USA). A 1.85 GBq (at calibration time) pharmaceutical grade gallium-68 generator (Eckert-Ziegler, Germany) has been used.  $^{68}\text{Ga}$ -IMP288 was obtained with a specific activity of 40 to 100 MBq/nmol with a radiochemical purity > 95%.

TF2 diluted in 250 mL 0.9% NaCl and  $^{68}\text{Ga}$ -IMP288 in 50 mL of 0.9% NaCl were administered by I.V. infusion over 30 minutes. Patients were premedicated with per os anti-histamine the day before TF2 infusion and with I.V. anti-histamine (polaramine) and corticosteroid (hydrocortisone hemisuccinate) 5 minutes before TF2 infusion. From patients 11 to 16, the same premedication was also administered before peptide infusion.

### **Study design**

Five pretargeting conditions were examined in five cohorts (C1 to C5) of 3 patients (Table 1). Safety was assessed by monitoring vital signs, physical examination and adverse events. For the 3-months follow-up, the imaging methods (CT, MRI,  $^{18}\text{F}$ -DOPA or  $^{18}\text{F}$ -FDG PET/CT) chosen to confirm abnormalities revealed by immuno-PET but not detected by baseline imaging were decided by a panel of experts involving endocrinologists, radiologists and nuclear physicians. A lesion detected by immuno-PET was considered related to MTC when confirmed by histology or detected by one other imaging modality and confirmed by the follow-up. HAHA was determined 3 and/or 6 months after TF2 infusion using an ELISA method (abnormal when  $\geq 50$  ng/mL).

### **PET/CT Imaging**

PET/CT was performed using a 4-ring Siemens Biograph mCT system with time of flight capability 60 and 120 min after  $^{68}\text{Ga}$ -IMP288 injection and reconstructed using a 3D ordinary

Poisson-OSEM with point-spread function correction and time of flight mode (3 iterations, 21 subsets, 2-mm full width at half maximum Gaussian post-filtering, voxel size: 4'4'2 mm<sup>3</sup>). Whole body acquisitions were performed under normal tidal respiration for 2.5 min per bed position. CT was obtained using a variable mAs, 120 kVp and a pitch of 1 without contrast enhancement. Acquisitions were performed from the top of the head to mid-thigh (6 to 8 steps per patient). Tumor SUV<sub>max</sub> (T-SUV<sub>max</sub>) was determined on the most intense focus in the whole-body scan confirmed as MTC according to the gold standard. Mediastinum blood pool SUV<sub>mean</sub> (MBP-SUV<sub>mean</sub>) was measured within a small volume of interest manually placed in the right atrium (V=1-2 cm<sup>3</sup>). The ratio T-SUV<sub>max</sub>/MBP-SUV<sub>mean</sub> (T/MBP) was subsequently calculated.

### **Pharmacokinetic Analysis**

Blood samples were collected before TF2 infusion, 5 min before the end of TF2 infusion and then 5 min, 1 and 2-4 h after infusion, and 5 min before the <sup>68</sup>Ga-IMP288 injection. TF2 concentrations were determined by ELISA. Blood samples were also collected 5 min, 1, 2 and 3-4 h after the <sup>68</sup>Ga-IMP288 injection, and counted immediately after the end of the blood collection, corrected for radioactive decay and transformed into molar concentrations.

Pharmacokinetic population modeling was performed using two-compartment models as described previously (17) .

### **RESULTS**

The characteristics of the 16 included patients are presented in Table 2. One of them did not receive the full hapten dose and was excluded. Fifteen patients (3 per cohort) were thus analyzed. No patient experienced an anaphylactic reaction during or after TF2 infusion. One patient experienced grade 3 reaction starting immediately after hapten infusion with malaise, bronchospasm, tachycardia and hypertension requiring hospitalization. HAHA analyzed in 11 patients (at 3 and 6 mo in 9 and only at 3 mo in 2) was abnormal in 2 patients, equal to 52 ng/ml at 3 mo and normalized at 6 months in one, and normal at 3 months and abnormal at 6 months (244 ng/mL) in the other.

Immuno-PET revealed abnormal foci in all patients, confirmed as MTC in 14 of them (Table 3). In patient 16, immuno-PET detected one neck focus not confirmed by conventional imaging or  $^{18}\text{F}$ -DOPA PET/CT at the time of the analysis. Figure 1 presents one example of immuno-PET in each cohort, and table 4 semi-quantitative analysis results. In cohort 1,  $\text{T-SUV}_{\text{max}}$  ranged from 4.1 to 8.9 at 60 min; tumor uptake and T/MBP increased for the 3 patients between 60 and 120 min. Considering MBP uptake in cohort 1 as too high, the delay was increased to 30 h in cohort 2, increasing  $\text{T-SUV}_{\text{max}}$  and T/MBP. Only one patient showed an increase of tumor uptake and contrast between 60 and 120 min. Because of the improvement between cohort 2 and cohort 1, the delay was further increased to 42 h in cohort 3, decreasing of  $\text{T-SUV}_{\text{max}}$  and contrast. Thus, the 30-h pretargeting delay appeared to be the most favorable. In cohort 4, the pretargeting delay was set back to 30 h and the TF2/peptide mole ratio was increased to 40 by injection of a lower IMP288 dose (3 nmol). With this schedule, high  $\text{T-SUV}_{\text{max}}$  was obtained, but with higher  $\text{MBP-SUV}_{\text{mean}}$  than in cohort 2. Tumor uptake and contrast increased in the 3 patients between 60 and 120 min. A reduced TF2 dose was tested in cohort 5, resulting in high tumor uptake in two patients but also in relatively high MBP, with increase of tumor uptake and contrast between 60 and 120 min. In contrast, blood activity was very low in patient 16.

TF2 pharmacokinetics was well described by a two-compartment model according to the population approach (Fig. 2 and Supplemental Table 1), but due to the short sampling time span, limited by the low injected dose and the limited sensitivity of the ELISA assay, the estimation of the  $\text{T}_{1/2}$  of the beta phase was not good for two patients (3 and 16). TF2 clearance was fast, estimated at  $0.6 \pm 0.1$  L/h, with a  $\text{T}_{1/2}$  of the alpha phase of  $4.1 \pm 0.5$  h. The  $\text{T}_{1/2}$  of the beta phase, after exclusion of the two outliers, was  $14.3 \pm 1.2$  h. The inter-individual variability was limited and explained in part by body surface (BS) differences: the coefficient of variation of the estimations of central compartment volume ( $V_c$ ) was reduced from 11.0% to 3.4% if reported by BS. As a result of the fast clearance, the concentrations of circulating TF2 at the time of hapten injection changed dramatically from 24 to 42 h (Fig. 2).

IMP288 pharmacokinetics was also well represented by a two-compartment model (Fig. 3 and Supplemental Table 2). Circulating TF2 is expected to bind the hapten and to reduce its clearance and the mean cohort clearances seemed to increase with the increase of time delay (C1:  $1.2 \pm 0.1$  L/h; C2:  $2.1 \pm 0.6$  L/h; C3:  $2.6 \pm 0.5$  L/h) for the same molar doses of TF2 (120 nmol) and IMP288 (6 nmol). Similarly, reducing the IMP288 dose to 3 nmol decreased its clearance (C4:  $1.0 \pm 0.5$  L/h). In cohort 5, with a TF2 dose reduced to 60 nmol, patients 14 and 15 showed a relatively slow TF2 clearance (0.46 and 0.36 L/h) and patient 16 a faster clearance (0.7 L/h). As a result, TF2 concentrations were high in patients 14 and 15, explaining the slower IMP288 clearances (0.54 and 0.7 L/h) and the high MBP on immuno-PET, and low for patient 16 explained in part by fast IMP288 clearance (5.4 L/h). Overall, a good correlation ( $R^2 = 0.9$ ) was obtained between IMP288 clearance and the circulating molar amount of TF2 at the time of peptide injection (Fig. 4A). The correlation between this molar ratio and SUVmax was not as good (Fig. 4B).

## DISCUSSION

This study is the first-in-human demonstration of the feasibility of pretargeted immuno-PET using the trivalent humanized TF2 BsMAb and  $^{68}\text{Ga}$ -IMP288 peptide. The previous clinical study assessing TF2 and  $^{177}\text{Lu}$ -IMP288 in metastatic colo-rectal patients showed selective tumor uptake within 1 h of peptide injection and high tumor-to-tissue uptake ratios at 24 h. The best tumor targeting was achieved with a 24 h-pretargeting interval, a high TF2 dose (150 mg, 955 nmol) and a very low (25  $\mu\text{g}$ , 17.5 nmol) peptide dose (14). Pre-pretargeting radioimmunotherapy (pRIT)  $^{111}\text{In}$ -IMP288 immunoscintigraphy showed good tumor targeting with a better contrast when the IMP288 dose was reduced. In our pRIT study assessing the same compounds in lung cancer patients, very similar conclusions were reached with regard to the best pretargeting conditions: a pretargeting delay of 24 h, a TF2 dose of 480 nmol/m<sup>2</sup> and an IMP288 dose of 24 nmol/m<sup>2</sup> (17). However the constraints for therapy and imaging are different: for therapy the injected activity must be high, which sets a minimum for the amount of injected IMP288, and the dose to the tumor must be maximum, not necessarily the tumor/organ ratios. The population pharmacokinetics analysis of this immuno-PET study showed a good correlation

between IMP288 clearance and the molar ratio of injected IMP288 to circulating TF2 at the time of IMP288 injection. This means that increasing the molar dose of IMP288 or the pretargeting delay will increase IMP288 clearance. Moreover, if the correlation between this molar ratio and SUV<sub>max</sub> was not as good as that of IMP288 clearance, the expected trend of lower tumor uptake for higher ratio was observed. Thus, a faster clearance of activity reduces background, but also reduces tumor uptake and the optimum that may be achieved.

According to a PET visual and semi-quantitative analysis, the 30-h pretargeting delay seemed to be the most favorable. Moreover, even if good imaging performances were observed in cohorts C2 and C4 using 120 nmol of TF2 and 30-h pretargeting delay, a TF2/IMP288 molar ratio of 20 in C2 appeared better than 40 in C4. Indeed, even if tumor uptake appeared to be higher, with the 40-molar ratio, with tumor SUV<sub>max</sub> increasing in the 3 patients between 60 and 120 min, the blood activity also seemed higher as shown by concordant semi-quantitative PET (higher MBP uptake in C4 than in C2) and pharmacokinetics results (decrease of hapten clearance), because the higher TF2 blood concentration causes a more efficient formation of peptide-BsMAb complexes (14,15). This relatively high blood activity diminishes tumor detectability, as shown in Figure 1. However, the increase of tumor uptake between 60 and 120 min in C4 suggests that a longer half-life PET emitter allowing later PET imaging, would be more favorable than <sup>68</sup>Ga for a 40-molar dose ratio. If a hapten radiolabeling with <sup>18</sup>F could also be envisaged using IMP449, this peptide is not currently available for clinical use. Moreover <sup>64</sup>Cu (half-life of 12.7 h) should be preferred allowing delayed images up to 48 hours after the hapten injection (18-19). “Moreover, the reduced peptide dose makes the labeling more difficult, requiring high specific activity, which may not be achieved at the end of the life of the gallium-68 generator.

Cohort 5 was set to test if a lower dose (60 nmol) of TF2 could give similar imaging performance. A large pharmacokinetic variability, in agreement with semi-quantitative PET observations, was observed in this cohort. Schoffelen et al. also described a considerable variability in IMP288 blood residence times in patients who received the lowest TF2 and IMP288 doses, despite a favorable imaging contrast (14,15). In cohort 5, patients 14 and 15 showed

good tumor uptake but also high MBP concordant with slow TF2 and hapten clearances. The image contrast was not optimal and was improved by later PET imaging with increased tumor uptake and T/MBP ratio between 60 and 120 min. By contrast, patient 16 showed fast TF2 and hapten clearances, concordant with the low MBP activity. High blood CEA concentration could accelerate the clearance of anti-CEA immunoglobulin because of antigen-antibody complexes formed in serum (20), but the plasma CEA concentration was low (3 ng/ml) in this patient. The only clinically relevant parameter register in this patient was a primary polycythemia diagnosed in the weeks after the immuno-PET. Thus, the cohort 2 protocol (120 nmol of TF2, 6 nmol of IMP288 and 30-h pretargeting delay) was considered the most favorable for PET imaging and the most reproducible in clinical practice.

This study confirmed the hypothesis previously proposed in our pRIT study that systematic I.V. injection of corticosteroids and antihistamines before TF2 injection may induce transient immunosuppression limiting immediate and delayed immune effects. No immediate immune effects were reported during or after TF2 infusion, and the immunization rate in our 2 studies (3/19) was lower than previously described by Schoffelen et al. (11/21) using the same compounds (14,15). A grade 3 adverse event was observed immediately after the IMP288 infusion suggesting an immune reaction to hapten as previously described using di-DTPA-indium hapten (16). Therefore, the protocol was amended and a premedication with antihistamine and corticosteroid prior to both TF2 and IMP288 injections was given to all patients. The low immunogenicity observed under these conditions also represents a favorable element for the use of immuno-PET as a theranostic approach, for example to select patients for pRIT.

Pretargeted immuno-PET detected MTC foci in all patients except one. The sensitivity of the technique will be evaluated in the second part of the study but these preliminary results already suggest that high tumor contrast can be obtained using this novel whole-body imaging. Our previous studies showed that CEA expression seemed to be almost constant in MTC, and that high sensitivity PET imaging using CEA as a target would detect the disease independently of the prognosis, in contrast to  $^{18}\text{F}$ FDG or  $^{18}\text{F}$ -DOPA PET/CT (4–6). Moreover, based on the lung

cancer pRIT study, we estimate that the induced internal radiation exposure resulting from  $^{68}\text{Ga}$ -IMP288 injection is very low with an effective dose obtained using MIRD S factors of  $1.9 \pm 1.2$  mSv equivalent to  $^{18}\text{F}$ FDG, which was estimated to be 2.3 mSv for the same injected activity (21).

An increased interest for immuno-PET is found in the recent literature (9,10), where targeted therapies using antibodies are experiencing a considerable growth in cancer management. Based on immuno-PET, treatment strategies could be tailored for individual patients before administering expensive and potentially toxic therapies. Immuno-PET can offer a non-invasive solution to quantitatively assess target expression. For example, anti-Her2 therapeutic agents are only effective in patients who have Her2-positive breast cancer, and immunoconjugates labeled with  $^{68}\text{Ga}$ ,  $^{64}\text{Cu}$  or  $^{89}\text{Zr}$  could non-invasively identify lesions that are likely to respond to therapy (19,22,23). Pretargeted immuno-PET could be a specific diagnostic tool for tumor detection but also a theranostic/companion approach to select patients to be treated with radioimmunconjugates or antibody-drug conjugates (ADC).

## **CONCLUSION**

This clinical study demonstrated the feasibility of immuno-PET using the anti-CEA humanized trivalent BsMab TF2 and the  $^{68}\text{Ga}$ -IMP288 hapten. We determined that 120 nmol of TF2, 6 nmol of peptide and a 30-h pretargeting delay seemed to be the best parameters for clinical practice. The sensitivity of this novel imaging method in relapsing MTC patients, in comparison with conventional imaging, will be assessed in the second part of the study, but present results already show that high contrast tumor uptake can be obtained.

## **ACKNOWLEDGMENTS**

This work was supported by grants from the French DHOS INCA in 2010, the French National Agency for Research, IRON Labex ANR-11-LABX-0018-01 and ArronaxPlus Equipex ANR-11-EQPX-0004. TF2 and IMP288 were provided by Immunomedics, Inc., and IBC Pharmaceuticals, Inc

## REFERENCES

1. Machens A, Schneyer U, Holzhausen H-J, Dralle H. Prospects of remission in medullary thyroid carcinoma according to basal calcitonin level. *J Clin Endocrinol Metab.* 2005;90:2029-2034.
2. Wells SA, Asa SL, Dralle H, et al. Revised American Thyroid Association guidelines for the management of medullary thyroid carcinoma. *Thyroid.* 2015;25:567-610.
3. Luster M, Karges W, Zeich K, et al. Clinical value of 18-fluorine-fluorodihydroxyphenylalanine positron emission tomography/computed tomography in the follow-up of medullary thyroid carcinoma. *Thyroid.* 2010;20:527-533.
4. Kauhanen S, Schalin-Jääntti C, Seppänen M, et al. Complementary roles of 18F-DOPA PET/CT and 18F-FDG PET/CT in medullary thyroid cancer. *J Nucl Med.* 2011;52:1855-1863.
5. Oudoux A, Salaun P-Y, Bournaud C, et al. Sensitivity and prognostic value of positron emission tomography with F-18-fluorodeoxyglucose and sensitivity of immunoscintigraphy in patients with medullary thyroid carcinoma treated with anticarcinoembryonic antigen-targeted radioimmunotherapy. *J Clin Endocrinol Metab.* 2007;92:4590-4597.
6. Verbeek HHG, Plukker JTM, Koopmans KP, et al. Clinical relevance of <sup>18</sup>F-FDG PET and 18F-DOPA PET in recurrent medullary thyroid carcinoma. *J Nucl Med.* 2012;53:1863-1871.
7. Peltier P, Curtet C, Chatal JF, et al. Radioimmunodetection of medullary thyroid cancer using a bispecific anti-CEA/anti-indium-DTPA antibody and an indium-111-labeled DTPA dimer. *J Nucl Med.* 1993;34:1267-1273.
8. Barbet J, Peltier P, Bardet S, et al. Radioimmunodetection of medullary thyroid carcinoma using indium-111 bivalent hapten and anti-CEA x anti-DTPA-indium bispecific antibody. *J Nucl Med* 1998;39:1172-1178.
9. Wu AM. Antibodies and antimatter: the resurgence of immuno-PET. *J Nucl Med.* 2009;50:2-5.
10. Boerman OC, Oyen WJG. Immuno-PET of cancer: a revival of antibody imaging. *J Nucl Med.* 2011;52:1171-1172.
11. Rossi EA, Goldenberg DM, Cardillo TM, McBride WJ, Sharkey RM, Chang C-H. Stably tethered multifunctional structures of defined composition made by the dock and lock method for use in cancer targeting. *Proc Natl Acad Sci U S A.* 2006;103:6841-6846.
12. McBride WJ, Zanzonico P, Sharkey RM, et al. Bispecific antibody pretargeting PET (immunoPET) with an <sup>124</sup>I-labeled hapten-peptide. *J Nucl Med.* 2006;47:1678-1688.

13. Schoffelen R, Sharkey RM, Goldenberg DM, et al. Pretargeted immuno-positron emission tomography imaging of carcinoembryonic antigen-expressing tumors with a bispecific antibody and a  $^{68}\text{Ga}$ - and  $^{18}\text{F}$ -labeled hapten peptide in mice with human tumor xenografts. *Mol Cancer Ther.* 2010;9:1019-1027.
14. Schoffelen R, Boerman OC, Goldenberg DM, et al. Development of an imaging-guided CEA-pretargeted radionuclide treatment of advanced colorectal cancer: first clinical results. *Br J Cancer.* 2013;109:934-942.
15. Schoffelen R, Woliner-van der Weg W, Visser EP, et al. Predictive patient-specific dosimetry and individualized dosing of pretargeted radioimmunotherapy in patients with advanced colorectal cancer. *Eur J Nucl Med Mol Imaging.* 2014;41:1593-1602.
16. Kraeber-Bodéré F, Rousseau C, Bodet-Milin C, et al. Targeting, toxicity, and efficacy of 2-step, pretargeted radioimmunotherapy using a chimeric bispecific antibody and  $^{131}\text{I}$ -labeled bivalent hapten in a phase I optimization clinical trial. *J Nucl Med.* 2006;47:247-255.
17. Bodet-Milin C, Ferrer L, Rauscher A, et al. Pharmacokinetics and dosimetry studies for optimization of pretargeted radioimmunotherapy in CEA expressing advanced lung cancer patient. *Front Med (Lausanne).* 2015;2:84.
18. McBride WJ, Sharkey RM, Karacay H, et al. A novel method of  $^{18}\text{F}$  radiolabeling for PET. *J Nucl Med.* 2009;50:991-998.
19. Tamura K, Kurihara H, Yonemori K, et al.  $^{64}\text{Cu}$ -DOTA-trastuzumab PET imaging in patients with HER2-positive breast cancer. *J Nucl Med.* 2013;54:1869-1875.
20. Sharkey RM, McBride WJ, Karacay H, et al. A universal pretargeting system for cancer detection and therapy using bispecific antibody. *Cancer Res.* 2003;63:354-363.
21. Andersson M, Johansson L, Minarik D, Leide-Svegborn S, Mattsson S. Effective dose to adult patients from 338 radiopharmaceuticals estimated using ICRP biokinetic data, ICRP/ICRU computational reference phantoms and ICRP 2007 tissue weighting factors. *EJNMMI Phys.* 2014;1:9.
22. Dijkers EC, Oude Munnink TH, Kosterink JG, et al. Biodistribution of  $^{89}\text{Zr}$ -trastuzumab and PET imaging of HER2-positive lesions in patients with metastatic breast cancer. *Clin Pharmacol Ther.* 2010;87:586-592.
23. Baum RP, Prasad V, Müller D, et al. Molecular imaging of HER2-expressing malignant tumors in breast cancer patients using synthetic  $^{111}\text{In}$ - or  $^{68}\text{Ga}$ -labeled affibody molecules. *J Nucl Med.* 2010;51:892-897.

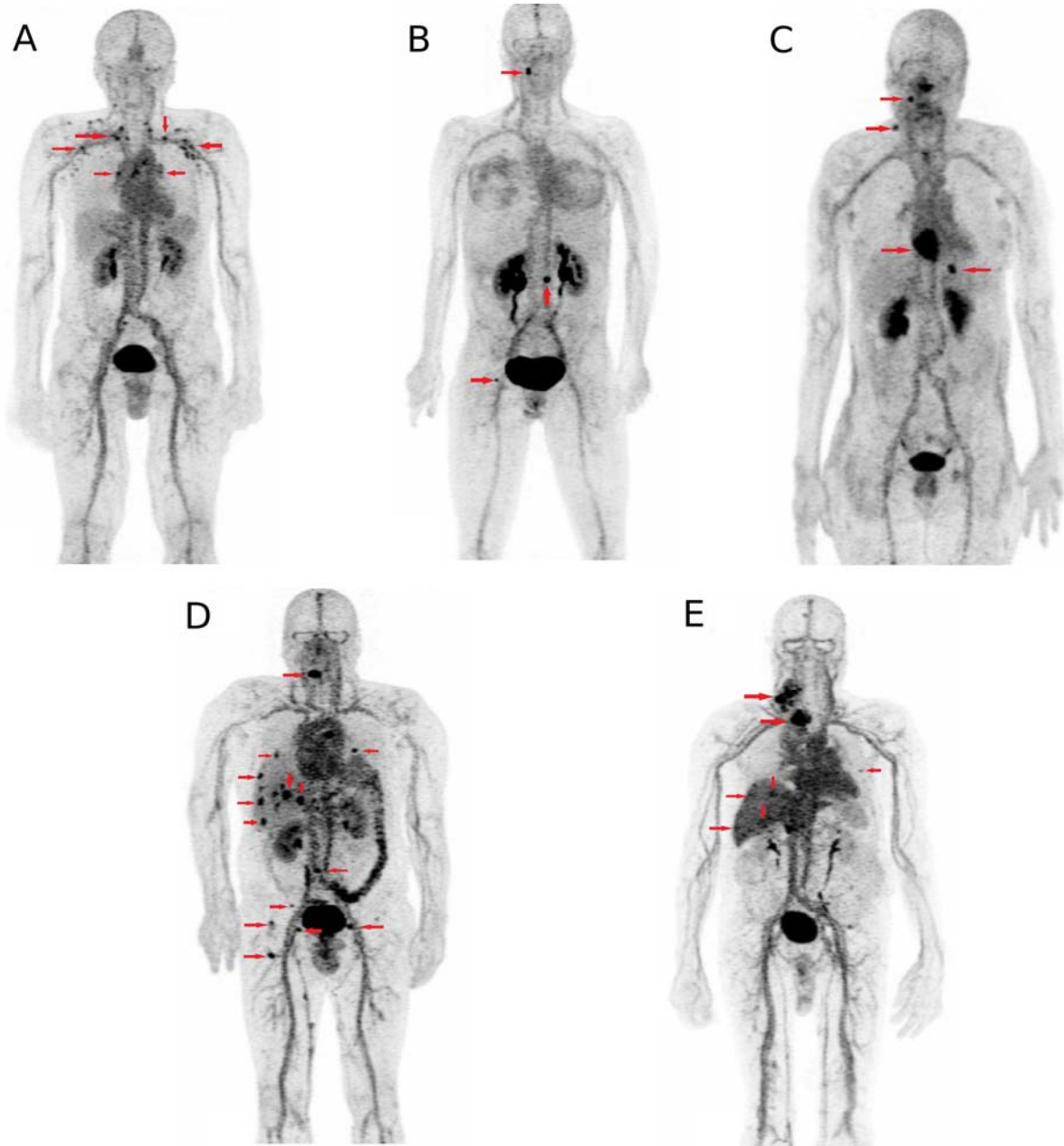


**FIGURE 1:** Immuno-PET MIP images recorded in one patient of each cohort. The arrows showed the foci considered as pathologic by immuno-PET: supra-diaphragmatic nodes in C1 (A ) cervical node, lumbar and femoral bones foci in C2 (B), supra-diaphragmatic nodes, liver and heart lesions in C3 (C), supra-diaphragmatic nodes, lung, liver and bone foci in C4 (D), and supra-diaphragmatic nodes and liver foci in C5 (E).

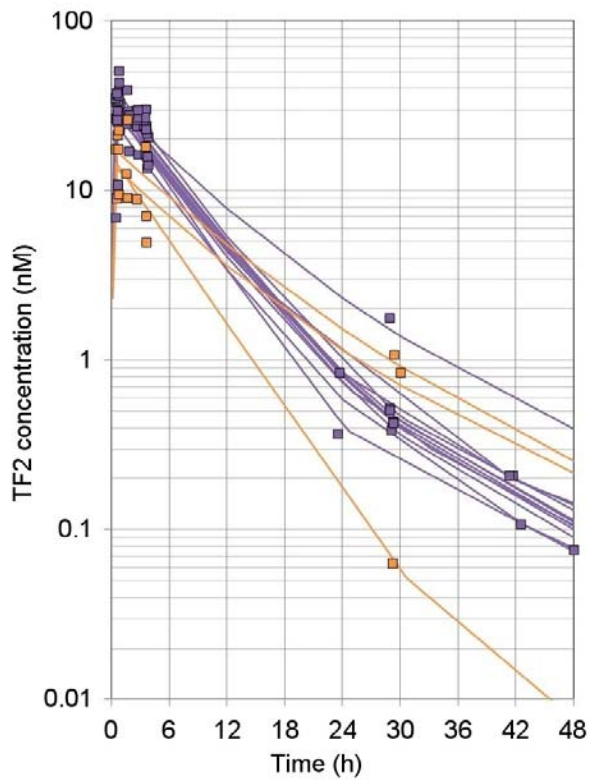


**FIGURE 2.** Pharmacokinetics of the bispecific antibody TF2. Patient received infusion of 60 (brown) or 120 nmol (purple) of TF2.

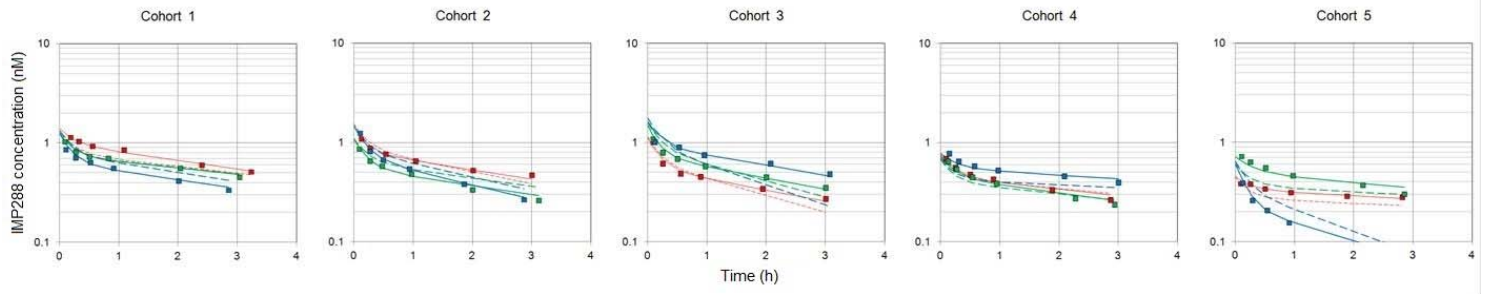


**FIGURE 3.** Pharmacokinetics of  $^{68}\text{Ga}$ -IMP288. Results are plotted as a semi-log plot with the population (dashed lines) and individual (solid lines) fitted curves.

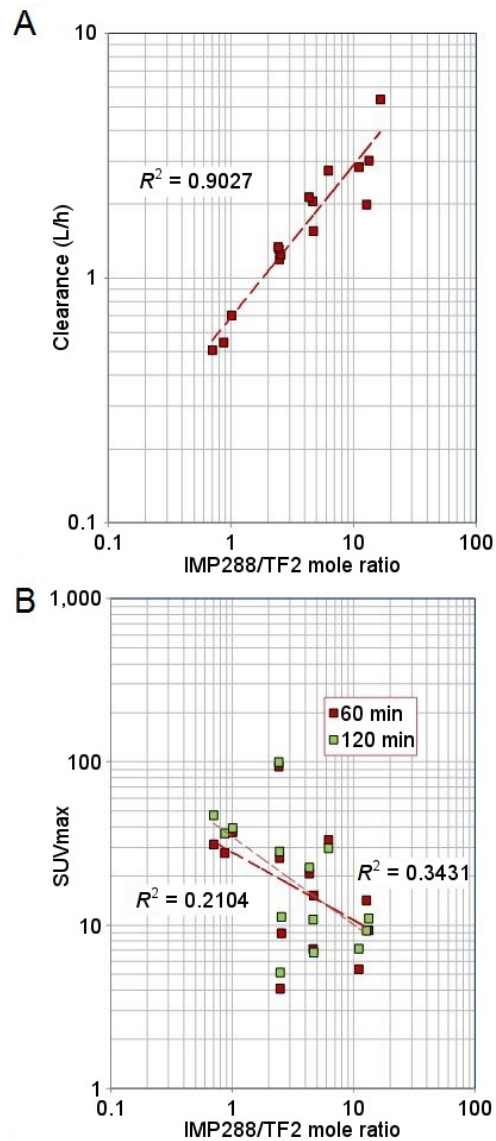


**FIGURE 4.** Correlation between IMP288 clearance (A) or SUVmax (B) and IMP228 to TF2 ratio. IMP288 clearance (A), estimated for each patient according to the population PK analysis, or SUVmax (B) were plotted (log-log plot) against the ratio of the number of moles of injected IMP288 to the number of moles of TF2 present in the circulation at the time of IMP288 injection. Correlation coefficients for the power function regression (dotted lines) are shown in the figure.

**TABLE 1**

Scheme of the cohorts.

	TF2 dose	delay	<sup>68</sup> Ga-IMP288 dose and activity	TF2/IMP288 molar dose ratio
Cohort I	120 nmol	24h	6 nmol 150 MBq	20
Cohort II	120 nmol	30h	6 nmol 150 MBq	20
Cohort III	120 nmol	42h	6 nmol 150 MBq	20
Cohort IV	120 nmol	30h	3 nmol 150 MBq	40
Cohort V	60 nmol	30h	3 nmol 150 MBq	20

**TABLE 2**

Patient Characteristics (n=16).

Median age in years (range)	60.5 (37-75)
Sex, <i>n</i> (%)	
Male	8(50)
Women	8 (50)
Median time from diagnosis in years (range)	8.5 (0.5-30 years)
Prior treatment, <i>n</i> (%)	
Surgery	15 (94)
External radiotherapy	4(25)
Radioimmunotherapy	2 (13)
Tyrosin kinase inhibitors	1 (6)
Median calcitonin concentration in pg/ml (range)	850 (154-39290)
Median CEA concentration in ng/ml (range)	22.5 (3-1443)
Median calcitonin doubling time in years (range)	1.3 (0.5-4.7)
Median CEA doubling time in years (range)	0.9 (0.6-4.4)
Location of disease, <i>n</i> (%)	
Lymph node	14 (88)
Lung	5 (32)
Liver	7 (44)
Bone	9 (56)
Other	2 (13)

**TABLE 3**

Number of confirmed lesions according the gold standard detected by immuno-PET, <sup>18</sup>F-DOPA PET/CT and conventional imaging for each patient.

Patient N°	Number of confirmed lesions according Gold Standard	Immuno-PET results		Number of lesions detected by <sup>18</sup> F-DOPA	Number of lesions detected by conventional imaging
		Number of lesions	Tumor SUV <sub>max</sub> range at 60 minutes		
1	2	2	3.6 and 4.1	1	1
2	13	13	2,7-8,9	6	10
3	6	6	1.2-7.2	3	6
4	8	6	2.8-15.3	7	5
5	7	7	4.1-20.8	6	4
6	2	2	15.1 and 33.3	2	1
7	14	14	2.9-12.5	12	11
9	8	7	3,5-5,4	3	8
10	4	4	2.2-12.9	1	4
11	9	7	4.9-25.8	4	8
12	14	12	5.3-94.1	12	13
13	1	1	31.3	1	0
14	8	8	6,9-27,7	6	6
15	6	5	3.2-37.1	5	6
16	0	0	-	0	0

Abbreviations: SUV, Standardized uptake value

**TABLE 4**

Semi-quantitative immuno-PET analysis.

	Tumor SUV <sub>max</sub>		MBP SUV <sub>mean</sub>		Tumor/MBP ratio	
	60 min	120 min	60 min	120 min	60 min	120 min
<b>Cohort 1</b>						
Patient 1	4.1	5.1	2.9	1.9	1.4	2.7
Patient 2	8.9	11.3	2.4	2.1	3.7	5.4
Patient 3	7.2	10.8	2.3	2.3	3.1	4.6
<b>Cohort 2</b>						
Patient 4	15.3	6.8	2.4	3.2	6.4	2.1
Patient 5	20.8	22.6	2.4	1.8	8.5	12.5
Patient 6	33.3	29.7	1.3	1.3	26.2	23.6
<b>Cohort 3</b>						
Patient 7	12.5	14.4	1.7	1.5	7.2	9.3
Patient 9	5.4	7.2	2.0	1.5	2.7	4.8
Patient 10	12.9	9.3	2.4	1.1	5.3	8.5
<b>Cohort 4</b>						
Patient 11	25.8	28.4	3.1	2.4	8.4	12.1
Patient 12	94.1	100.2	2.8	2.0	34.1	49.6
Patient 13	31.3	47.2	4.5	3.9	6.9	12.2
<b>Cohort 5</b>						
Patient 14	27.7	36.6	4.9	4.7	5.6	7.7
Patient 15	37.1	39.4	4.0	3.3	9.3	11.8
Patient 16	ND	ND	0.7	0.5	ND	ND
Abbreviations: SUV, Standardized uptake value; MBP, mediastinal blood pool; ND, not defined.						